



Published in final edited form as:

*Arch Biochem Biophys.* 2012 September 1; 525(1): 1–8. doi:10.1016/j.abb.2012.05.024.

## Alanine or aspartic acid substitutions at serine23/24 of cardiac troponin I decrease thin filament activation, with no effect on crossbridge detachment kinetics

Ranganath Mamidi, Sampath K. Gollapudi, Sri Lakshmi Mallampalli, and Murali Chandra  
Department of Veterinary and Comparative Anatomy, Pharmacology, and Physiology (VCAPP),  
Washington State University, Pullman, Washington

### Abstract

Ala/Asp substitutions at Ser23/24 have been employed to investigate the functional impact of cardiac troponin I (cTnI) phosphorylation by protein kinase A (PKA). Some limitations of previous studies include the use of heterologous proteins and confounding effects arising from phosphorylation of cardiac myosin binding protein-C. Our goal was to probe the effects of cTnI phosphorylation using a homologous assay, so that altered function could be solely attributed to changes in cTnI. We reconstituted detergent-skinned rat cardiac papillary fibers with homologous rat cardiac troponin subunits to study the impact of Ala and Asp substitutions at Ser23/24 of rat cTnI (RcTnI S23A/24A and RcTnI S23D/24D). Both RcTnI S23A/24A and RcTnI S23D/24D showed a ~36% decrease in Ca<sup>2+</sup>-activated maximal tension. Both RcTnI S23A/24A and RcTnI S23D/24D showed a ~18% decrease in ATPase activity. Muscle fiber stiffness measurements suggested that the decrease in thin filament activation observed in RcTnI S23A/24A and RcTnI S23D/24D was due to a decrease in the number of strongly-bound crossbridges. Another major finding was that Ala and Asp substitutions in cTnI did not affect crossbridge detachment kinetics.

### Keywords

Cardiac troponin I; phosphorylation; substitutions; reconstitution; homologous proteins

## INTRODUCTION

Protein Kinase A (PKA)-mediated phosphorylation of cardiac troponin I (cTnI) enhances cardiac function during  $\beta$ -adrenergic stimulation [1, 2]. When phosphorylated by PKA, the hydroxyl groups of Ser23/24 in cTnI are replaced by negatively-charged phosphate groups [3]. Because the pK value of a phosphoserine falls within the range of 6.5–7.5, PKA-mediated phosphorylation of cTnI most likely generates a total of 3 negative charges at or near physiological pH. The incorporation of negatively-charged phosphate groups induces intra-molecular interactions between Ser24 and other amino acids in cTnI [3]. Such structural changes in cTnI are linked to its effects on decreased myofilament Ca<sup>2+</sup> sensitivity

© 2012 Elsevier Inc. All rights reserved.

Corresponding author/address for reprints: Murali Chandra, Ph.D., Dept. of VCAPP, 205 Wegner Hall, Washington State University, Pullman, WA 99164-6520, Phone: (509) 335-7561, Fax: (509) 335-4650, murali@vetmed.wsu.edu.

**Publisher's Disclaimer:** This is a PDF file of an unedited manuscript that has been accepted for publication. As a service to our customers we are providing this early version of the manuscript. The manuscript will undergo copyediting, typesetting, and review of the resulting proof before it is published in its final citable form. Please note that during the production process errors may be discovered which could affect the content, and all legal disclaimers that apply to the journal pertain.

[2, 4], decreased affinity of cTnI to cardiac troponin C (cTnC) [5], and increased crossbridge (XB) detachment kinetics [6, 7].

Diverse experimental approaches have been used to understand the functional consequences of PKA-mediated phosphorylation of Ser23/24 in cTnI. One commonly used approach is the treatment of detergent-skinned rat cardiac myocytes and trabeculae with the catalytic subunit of PKA [8–10]. However, there are some limitations associated with the experimental conditions employed in such studies. For example, the extent of cTnI phosphorylation by the catalytic subunit of PKA in skinned cardiac fibers may vary from that observed during *in vivo*  $\beta$ -adrenergic stimulation - such variations, when coupled with the confounding effects of PKA-mediated phosphorylation of cardiac myosin binding protein-C (cMyBP-C) [8], are likely to add ambiguity to data interpretations.

In transgenic (TG) mouse studies, two different approaches have been used. In the first TG approach, murine slow skeletal TnI [4, 11] or rat cTnI [12] were expressed in the mouse heart. The use of proteins from different species and tissues - which contain significant sequence heterogeneity - is likely to introduce ambiguity in the inferences drawn from such TG mouse studies. In the second TG approach, mouse cTnI mutants were expressed in the mouse heart [13, 14]. Although the second approach used a homologous protein, it was difficult to tease apart the functional effects of PKA-mediated phosphorylation of cTnI from that of cMyBP-C [13, 14]. To avoid such complications, several investigators have used *in vitro* reconstitution procedures to study the effect of cTnI phosphorylation. For example, skinned porcine cardiac muscle fibers were reconstituted with mouse cTnI containing Ala [15] or human cTnI containing Asp [16] substitutions at Ser23/24. The use of heterologous proteins such as mouse and human proteins in porcine cardiac tissue has the potential of complicating data interpretations.

In our study, we used a homologous assay where the observed functional alterations could be solely attributed to changes introduced in cTnI. Detergent-skinned rat cardiac papillary muscle fibers were reconstituted with the homologous rat cardiac troponin (Tn) subunits. Recombinant rat cTnI (RcTnI), in which Ser23/24 were substituted with either Ala (RcTnI S23A/24A) or Asp (RcTnI S23D/24D), was used in our reconstitution studies. Our results demonstrate that both Ala and Asp substitutions in cTnI decrease cardiac thin filament activation -  $\text{Ca}^{2+}$ -activated maximal tension, ATPase activity, and muscle fiber stiffness parameters were attenuated. Another major finding was that Ala and Asp substitutions in cTnI did not affect XB detachment kinetics.

## METHODS

### Animal protocols

Papillary muscle bundles were isolated from the left ventricles of hearts from young adult, male Sprague-Dawley rats. Rats used in this study received proper care and humane treatment according to the guidelines of the Washington State University Institutional Animal Care and Use Committee. All animals used in this study were properly handled to minimize the pain and suffering according to the procedures recommended by the animal use principles of the National Academy of Sciences Guide for the Care and Use of Laboratory Animals.

### Preparation of detergent-skinned cardiac muscle fiber bundles

Detergent-skinned left ventricular papillary muscle fiber bundles were prepared, as previously described [17, 18]. Briefly, rats were deeply anesthetized by inhalation of isoflurane. The depth of the anesthesia was assessed by a lack of pedal withdrawal reflex. Hearts were quickly removed and placed into an ice-cold high relaxing (HR) solution of pCa

9.0 containing: (in mM) 20 2, 3-butanedione monoxime (BDM), 50 N,N-bis (2-hydroxyethyl)-2-amino-ethane-sulfonic acid (BES), 20 EGTA, 6.29 MgCl<sub>2</sub>, 6.09 Na<sub>2</sub>ATP, 30.83 potassium propionate, 10 sodium azide, 1.0 DTT, and 4 benzamidine-HCl. The pH of the solution was adjusted to 7.0 with KOH. A fresh cocktail of protease inhibitors (in μM): 5 bestatin, 2 E-64, 10 leupeptin, 1 pepstatin, and 200 phenylmethylsulfonyl fluoride (PMSF) was added to the relaxing solution. Papillary muscle bundles were further dissected into smaller fiber bundles (fibers) of approximately 0.15 mm in width and 2 mm in length. Fibers were detergent-skinned overnight at 4°C in HR containing 1% Triton X-100.

### Expression and purification of recombinant rat cardiac Tn subunits

*c-myc* tagged recombinant rat cardiac troponin T (*c-myc* RcTnT), RcTnI, and rat cTnC (RcTnC), all cloned into pSBETa vector, were expressed in BL21\*DE3 cells (Novagen, Madison, WI) for protein synthesis. Ala and Asp substitutions in RcTnI (RcTnI S23A/24A and RcTnI S23D/24D) were generated using site-directed DNA mutagenesis techniques and cloned into pSBETa vector. *c-myc* RcTnT, RcTnI, and RcTnC were purified according to the methods described previously [18]. In brief, BL21\*DE3 cells were lysed and the proteins were purified using ion-exchange chromatography techniques. *c-myc* RcTnT was purified using a DEAE column, while RcTnC was purified using a DE-52 column. RcTnI, RcTnI S23A/24A, and RcTnI S23D/24D proteins were purified using a CM-Sepharose column. Eluted protein fractions were run on a 12.5% SDS-PAGE to evaluate their purity. Pure protein fractions were pooled, dialyzed thoroughly against deionized water containing 15 mM β-mercaptoethanol, and lyophilized.

### Reconstitution of recombinant rat cardiac Tn subunits into detergent-skinned rat cardiac muscle fibers

Reconstitution of recombinant Tn subunits into muscle fibers was carried out using a protocol described previously [18]. In brief, the extraction of native Tn subunits was carried out using an extraction solution containing a mixture of *c-myc* RcTnT and RcTnI proteins. *c-myc* RcTnT was used in our reconstitution procedure, so that the incorporation of exogenously added Tn subunits could be assessed using an antibody to *c-myc* epitope in RcTnT. It has been shown that the use of cTnT with an 11 amino acid *c-myc* epitope at the N-terminus do not affect normal cardiac function [19, 20]. Removal of the endogenous Tn subunits was carried out using an extraction solution containing *c-myc* RcTnT (1.5 mg/ml, W/V) and RcTnI (1.0 mg/ml, W/V) in 50 mM Tris-HCl (pH 8.0), 6 M urea, 1.0 M KCl, 10 mM DTT, and a cocktail of protease inhibitors. High salt and urea in the extraction solution was removed according to a protocol described previously [18]. Finally, the *c-myc* RcTnT-RcTnI treated fibers were incubated with RcTnC to complete the reconstitution procedure [18]. Detergent-skinned fibers reconstituted with *c-myc* RcTnT + RcTnI S23A/24A + RcTnC are referred to as “RcTnI S23A/24A” and those reconstituted with *c-myc* RcTnT + RcTnI S23D/24D + RcTnC are referred to as “RcTnI S23D/24D”. Fibers reconstituted with *c-myc* RcTnT + RcTnI + RcTnC are referred to as “RcTnI WT” and were used as controls.

The reconstituted fibers were resuspended in 2% SDS solution (10 μl/fiber) for SDS-PAGE [21]. SDS-digested fibers were mixed with an equal volume of protein loading dye, which contained 125 mM Tris-HCl (pH 6.8), 20% glycerol, 2% SDS, 0.01% bromophenol blue, and 50 mM β-mercaptoethanol. Equal quantities of protein (10 μg) from the digested fibers were loaded and separated on a SDS-PAGE (4% acrylamide stacking gel and 12.5% acrylamide separating gel). Proteins from SDS gel were transferred onto a PVDF membrane for the Western blot analysis. The incorporation of *c-myc* RcTnT was assessed using a horseradish peroxidase (HRP)-labeled antibody to the *c-myc* epitope (Santa Cruz Biotechnology, clone #9E10) [19, 20]. The incorporation of RcTnI was assessed using an anti-TnI primary antibody (Abcam, clone #284[19C7]), followed by a HRP-labeled anti-mouse secondary

antibody (Amersham Biosciences). The incorporation of RcTnC was assessed using an anti-TnC primary antibody (Fitzgerald, clone #M5092922), followed by a HRP-labeled anti-mouse secondary antibody (Amersham Biosciences). To compare protein band intensities in different groups of fibers, densitometric scanning of Western blots was performed using Image J software (acquired from NIH at: <http://rsbweb.nih.gov/ij/>). The relative incorporation of exogenously-added Tn subunits was determined by calculating the percentage band intensity for RcTnI S23A/24A and RcTnI S23D/24D vs. that observed for the RcTnI WT reconstituted fibers.

### **Estimation of protein secondary structure using far-UV circular dichroism (far-UV CD) spectroscopy**

Far-UV CD spectra for RcTnI, RcTnI S23A/24A, and RcTnI S23D/24D proteins were collected in the range of 200 nm-240 nm using an Aviv 202 SF CD spectrometer [22]. Purified proteins were dissolved in a solution containing 6 M urea, 50 mM Tris base, 1 M KCl, and 1 mM DTT (pH 8.0). A fresh cocktail of protease inhibitors - which contained 5 mM benzamidine-HCl, 0.4 mM PMSF, 10  $\mu$ M leupeptin, 1  $\mu$ M pepstatin, 5  $\mu$ M bestatin, and 2  $\mu$ M E-64 - was added to the urea solution. Dissolved protein samples were dialyzed overnight at 4°C against a phosphate buffer, which contained 0.2 M sodium phosphate monobasic, 0.2 M sodium phosphate dibasic, 0.5 M KCl, and 0.1 mM DTT (pH 7.0). Dialyzed protein samples were diluted with the phosphate buffer to achieve a final protein concentration of 10  $\mu$ M. CD spectra were collected for both the phosphate buffer and the protein samples. The net CD signals for the protein samples were calculated by extracting the CD signals of the phosphate buffer from the CD signals of the protein samples. The secondary-structural content of the protein samples was estimated by analyzing the far-UV CD spectral data using a K2D algorithm available on DICHROWEB, a web-based program to analyze CD spectral data [23, 24].

### **Simultaneous measurement of steady-state isometric force and ATPase activity**

Simultaneous measurement of isometric steady-state force and ATPase activity was according to a procedure described previously [8, 25]. In brief, T-shaped aluminum clips were used to secure the muscle fiber between the motor arm (322C, Aurora Scientific Inc) and the force transducer (AE 801, Sensor One Technologies Corp). The resting sarcomere length (SL) was set to 2.2  $\mu$ m using a laser diffraction pattern [8, 25]. The muscle fiber was immersed in a constantly-stirred chamber containing  $\text{Ca}^{2+}$  solutions, the concentration of which ranged from pCa of 4.3 to 9.0 (pCa = -log of free  $[\text{Ca}^{2+}]$ ). The composition of various pCa solutions was calculated using methods described previously [26]. The composition of the maximal  $\text{Ca}^{2+}$  activation solution (pCa 4.3) was: (in mM) 31 potassium propionate, 5.95  $\text{Na}_2\text{ATP}$ , 6.61  $\text{MgCl}_2$ , 10 EGTA, 10.11  $\text{CaCl}_2$ , 50 BES (pH 7.0), 5  $\text{NaN}_3$ , and 10 phosphoenol pyruvate (PEP). The composition of the relaxing solution (pCa 9.0) was: (in mM) 51.14 potassium propionate, 5.83  $\text{Na}_2\text{ATP}$ , 6.872  $\text{MgCl}_2$ , 10 EGTA, 0.024  $\text{CaCl}_2$ , 50 BES (pH 7.0), 5  $\text{NaN}_3$ , and 10 PEP. The activation and relaxing solutions also contained 0.5 mg/ml pyruvate kinase (500 U/mg), 0.05 mg/ml lactate dehydrogenase (870 U/mg), 20  $\mu$ M diadenosine pentaphosphate ( $\text{A}_2\text{P}_5$ ), 10  $\mu$ M oligomycin, and a cocktail of protease inhibitors. The pH was adjusted to 7.0 using KOH. The ionic strength was 180 mM. After two cycles of maximal activation and relaxation, the SL was monitored again and reset to 2.2  $\mu$ m if needed. The muscle fiber was then immersed in a series of  $\text{Ca}^{2+}$  solutions (pCa 4.3 to 9.0), and the isometric steady-state forces were digitally recorded on a computer.

Steady-state isometric ATPase activity was measured according to a protocol described previously [8, 25]. Briefly, near-UV light (340 nm) was projected through the muscle chamber, then split (50:50) via a beam splitter and detected at 340 nm (sensitive to changes in NADH) and at 400 nm (insensitive to changes in NADH). ATPase activity was measured

as follows: ATP regeneration from ADP was coupled to the breakdown of PEP to pyruvate and ATP catalyzed by pyruvate kinase, which was linked to the synthesis of lactate catalyzed by lactate dehydrogenase. The breakdown of NADH during the synthesis of lactate was proportional to the ATP consumption and was measured by changes in UV absorbance at 340 nm. The signal for NADH was calibrated by multiple injections of 0.25 nmol of ADP.

### Measurement of dynamic stiffness and the rate of XB detachment in reconstituted fibers

Once the muscle fiber reached the steady-state isometric force in pCa 4.3 solution, step-like length changes were applied to the muscle fiber [27]. During the steady-state isometric force, the motor arm was commanded to change the muscle length (ML) in a step-like pattern, where the increases and decreases in ML were in the order of 0.5%, 1.0%, 1.5%, and 2.0% of the initial ML. The ML was initially increased by 0.5% ML (stretched), held at the increased length for 5 seconds, and then the motor arm was commanded to rapidly return (released) to the initial ML. The same protocol was repeated for further step-like length changes of 1.0%, 1.5%, and 2.0% ML. To estimate the instantaneous muscle fiber stiffness and the rate of XB detachment kinetics, a nonlinear recruitment distortion (NLRD) model was fitted to the force responses elicited by changes in ML [27].

### Measurement of the maximal fiber shortening velocity ( $V_{max}$ ) in reconstituted fibers

$V_{max}$  was estimated using the force-velocity (F-V) relationships, which were measured using the force-ramp (F-R) protocol described previously [28]. Briefly, once the muscle fiber attained a steady-state isometric force at pCa 4.3, the F-R protocol and subsequent length changes were imposed and recorded for each fiber. The rate for the F-R was set to  $-2 F_0/\text{sec}$ ,  $F_0$  being the initial steady-state isometric force, and the fiber was shortened until the force (F) of the fiber was ramped down to zero. The active forces during F-R trial were calculated as the difference between the total and parallel passive forces. Fiber velocities were calculated by dividing the difference between the successive length data values with the sampling time interval. Force and shortening velocity were normalized to initial force,  $F_0$ , and initial fiber length,  $L_0$ , respectively. Normalized force and velocity were used to construct the F-V relationship. The Hill's hyperbolic equation was fitted to the active F-V relationship to extrapolate  $V_{max}$ , as the velocity at which the net force elicited by the fiber was zero.

### Data analysis

All data are shown as mean  $\pm$  SEM. pCa<sub>50</sub> (-log of free [Ca<sup>2+</sup>] required to elicit half maximal force) and cooperativity of tension development ( $n_H$ ) values were estimated by fitting the Hill equation to the pCa-tension data. Statistical differences between different groups of data were analyzed by one-way analysis of variance (ANOVA), followed by post hoc Fischer's LSD t-test, with substitutions in RcTnI as a factor responsible for the variance. The criterion for statistical significance was set at  $P < 0.05$ .

## RESULTS

### Western blot analysis of Tn subunits in reconstituted fibers

RcTnI WT, RcTnI S23A/24A, and RcTnI S23D/24D reconstituted fibers were digested using 2% SDS solution, as described previously [21]. Equal quantities of the digested fiber samples (10  $\mu\text{g}$  of protein per sample) were run on a 12.5% SDS gel to achieve molecular weight-based separation of the Tn subunits. After Western blotting with different antibodies (see methods), the Image J software was used to analyze the band intensities of Tn subunits in different lanes. The relative incorporation of *c-myc* RcTnT into RcTnI S23A/24A or

RcTnI S23D/24D fibers was 103% or 101%, respectively vs. that incorporated into RcTnI WT fibers (Figure 1A). The relative incorporation of RcTnI into RcTnI S23A/24A or RcTnI S23D/24D fibers was 102.5% or 99.6%, respectively vs. that incorporated into RcTnI WT fibers (Figure 1B). The relative incorporation of RcTnC into RcTnI S23A/24A or RcTnI S23D/24D fibers was 100.7% or 102%, respectively vs. that incorporated into RcTnI WT fibers (Figure 1C). Thus, results from our Western blot analysis demonstrate that the efficiency of incorporation of different Tn subunits is similar in all groups of reconstituted fibers.

### Effect of S23A/24A and S23D/24D substitutions on the overall secondary structure of RcTnI

PKA-mediated phosphorylation of cTnI introduces negatively-charged phosphate groups at Ser23 and Ser24. NMR studies [3] have demonstrated that these negatively-charged phosphate groups induce intra-molecular interactions between the side chains of Ser24 and Arg22, indicating that minor modifications at Ser23/24 alter cTnI structure. Therefore, the substitution of hydrophilic Ser residues with hydrophobic Ala or negatively-charged acidic Asp residues may affect the secondary structure of cTnI. To determine if substitutions at Ser23 and Ser24 caused any structural changes in cTnI, we measured far-UV CD spectral features of RcTnI, RcTnI S23A/24A, and RcTnI S23D/24D proteins. Results indicated that Ala or Asp substitutions did not induce any major alterations in the overall secondary structure of RcTnI. Unaltered secondary structure was indicated by the lack of statistical differences between the percentages of  $\alpha$ -helical,  $\beta$ -sheet, and random coil contents of RcTnI S23A/24A and RcTnI S23D/24D proteins when compared to that of RcTnI protein (Table 1).

### Effect of RcTnI S23A/24A and RcTnI S23D/24D on $\text{Ca}^{2+}$ -activated maximal tension and ATPase activity

First, we studied the effects of Ala and Asp substitutions on  $\text{Ca}^{2+}$ -activated maximal tension and ATPase activity in detergent-skinned rat cardiac fibers reconstituted with RcTnI WT, RcTnI S23A/24A, and RcTnI S23D/24D.  $\text{Ca}^{2+}$ -activated maximal tension (in  $\text{mN}\cdot\text{mm}^{-2}$ ) values were  $42.7 \pm 2.5$ ,  $29.3 \pm 1.9$ , and  $29.6 \pm 1.7$  in RcTnI WT, RcTnI S23A/24A, and RcTnI S23D/24D reconstituted fibers, respectively (Figure 2A). These values amounted to a ~36% decrease in tension in both RcTnI S23A/24A and RcTnI S23D/24D reconstituted fibers, when compared to RcTnI WT reconstituted fibers. Thus,  $\text{Ca}^{2+}$ -activated maximal tension decreased significantly due to S23A/24A and S23D/24D substitutions in cTnI. Maximal ATPase activity (in  $\text{pmol}\cdot\text{mm}^{-3}\cdot\text{s}^{-1}$ ) values were  $174.6 \pm 10.7$ ,  $145.1 \pm 6.5$ , and  $143.7 \pm 8.4$  in RcTnI WT, RcTnI S23A/24A, and RcTnI S23D/24D reconstituted fibers, respectively (Figure 2B). These values amounted to a ~18% decrease in ATPase activity in both RcTnI S23A/24A and RcTnI S23D/24D reconstituted fibers, when compared to RcTnI WT reconstituted fibers. Thus,  $\text{Ca}^{2+}$ -activated maximal ATPase activity decreased significantly due to S23A/24A and S23D/24D substitutions in cTnI. Collectively, these observations demonstrate that substitutions at S23/24 of cTnI, be it Ala or Asp, lead to a significant decrease in  $\text{Ca}^{2+}$ -activated maximal tension and ATPase activity.

### Effect of RcTnI S23A/24A and RcTnI S23D/24D on muscle fiber stiffness

To examine if the reduction in  $\text{Ca}^{2+}$ -activated maximal tension and ATPase activity were due to a decrease in the number of force-generating XBs, we measured the muscle fiber stiffness ( $E_D$ ) by imposing step-like length perturbations in constantly-activated muscle fibers.  $E_D$  is an index of stiffness of the population of bound XBs at the time of length change, and is proportional to the number of strongly-bound, force-generating XBs [27]. To estimate  $E_D$ , the NLRD model was fitted to the immediate force responses elicited by changes in ML. These changes in force responses ( $\Delta$  tension) were plotted against changes

in ML ( $\Delta L$ ). The stiffness relationships of these reconstituted fibers showed that the slopes of RcTnI S23A/24A and RcTnI S23D/24D reconstituted fibers deviated significantly from that of RcTnI WT reconstituted fibers (Figure 3A). The slope value, which is a measure of  $E_D$  (in  $\text{mN}\cdot\text{mm}^{-3}$ ), decreased significantly in fibers reconstituted with RcTnI S23A/24A ( $571.4 \pm 52.2$ ) or RcTnI S23D/24D ( $550.1 \pm 30.6$ ), when compared to fibers reconstituted with RcTnI WT ( $857.7 \pm 40.7$ ; Figure 3B). Because both tension (Figure 2A) and  $E_D$  (Figure 3) decreased similarly, the tension/stiffness ratio was similar in all groups of fibers. Thus, the tension per XB remained the same in all groups of fibers. Therefore, our data demonstrates that the attenuation of  $\text{Ca}^{2+}$ -activated maximal tension (Figure 2A) and ATPase activity (Figure 2B) in RcTnI S23A/24A or RcTnI S23D/24D fibers was due to reduced thin filament activation caused by a decrease in the number of force-generating XBs.

### Effect of RcTnI S23A/24A and RcTnI S23D/24D on the myofilament $\text{Ca}^{2+}$ sensitivity

The pCa-tension relationships in the reconstituted fibers were estimated by plotting the normalized tension values against a range of pCa (Figure 4). Hill's equation was fitted to the pCa-tension relationships to estimate myofilament  $\text{Ca}^{2+}$  sensitivity ( $\text{pCa}_{50}$ ) and cooperativity of tension development ( $n_H$ ).  $\text{pCa}_{50}$  values were  $5.46 \pm 0.01$ ,  $5.43 \pm 0.01$ , and  $5.37 \pm 0.02$  for RcTnI WT, RcTnI S23A/24A, and RcTnI S23D/24D reconstituted fibers, respectively. One-way ANOVA showed that  $\text{pCa}_{50}$  decreased significantly ( $P < 0.005$ ) in RcTnI S23D/24D reconstituted fibers, but it was unaltered in RcTnI S23A/24A reconstituted fibers (Figure 4). Thus, as for  $\text{Ca}^{2+}$  sensitivity, Asp substitution mimicked the  $\text{Ca}^{2+}$  desensitizing effect of PKA-mediated phosphorylation of cTnI.  $n_H$  values were  $3.60 \pm 0.09$ ,  $4.47 \pm 0.25$ , and  $4.55 \pm 0.29$  for RcTnI WT, RcTnI S23A/24A, and RcTnI S23D/24D reconstituted fibers, respectively. RcTnI S23A/24A and RcTnI S23D/24D reconstituted fibers showed a significant increase ( $P < 0.05$ ) in  $n_H$ , when compared to RcTnI WT reconstituted fibers.

### Effect of RcTnI S23A/24A and RcTnI S23D/24D on tension cost and the rate of XB detachment

To estimate tension cost values, the relationship between steady-state isometric tension and the corresponding ATPase activity was determined at various levels of  $\text{Ca}^{2+}$  activation [17, 18, 29]. Tension cost (in  $\text{pmol}\cdot\text{mN}^{-1}\cdot\text{mm}^{-1}\cdot\text{s}^{-1}$ ) values were:  $4.63 \pm 0.36$  for RcTnI WT;  $5.40 \pm 0.31$  for RcTnI S23A/24A; and  $5.41 \pm 0.31$  for RcTnI S23D/24D. One-way ANOVA showed that tension cost of fibers reconstituted with RcTnI S23A/24A or RcTnI S23D/24D was not significantly different from that of fibers reconstituted with RcTnI WT (Figure 5A). Because changes in tension cost reflects changes in the rate of XB detachment [30], our data demonstrates that the rate of XB detachment was not altered by either RcTnI S23A/24A or RcTnI S23D/24D.

Our results from tension cost experiments were supported by measurements of the rate of XB detachment kinetics, as estimated from the rate of XB distortion dynamics ( $c$ ). We have previously shown that there is a strong correlation between tension cost and  $c$  [31]. The estimates of  $c$  (in  $\text{s}^{-1}$ ) were:  $21.60 \pm 1.07$  for RcTnI WT;  $22.77 \pm 2.62$  for RcTnI S23A/24A; and  $26.69 \pm 2.46$  for RcTnI S23D/24D. One-way ANOVA showed that the NLRD model-estimated values of  $c$  were not significantly different between fibers reconstituted with RcTnI WT, RcTnI S23A/24A, and RcTnI S23D/24D (Figure 5B). Thus, unaltered tension cost and  $c$  suggest that Ala and Asp substitutions in RcTnI have no effect on the rate of XB detachment.

### Effect of RcTnI S23A/24A and RcTnI S23D/24D on maximal fiber shortening velocity ( $V_{\max}$ )

Another way to probe the rate of XB detachment is to measure  $V_{\max}$ . A force-ramp (F-R) protocol [28] was applied to constantly-activated muscle fibers to measure the force-velocity (F-V) relationships. Shortening velocities were plotted as a function of normalized force to determine the F-V relationships, and  $V_{\max}$  was estimated as the velocity at which the muscle fibers exhibited zero force. The values of  $V_{\max}$  (in  $L_0 \cdot s^{-1}$ ) for RcTnI WT, RcTnI S23A/24A, and RcTnI S23D/24D reconstituted fibers were  $1.89 \pm 0.06$ ,  $2.25 \pm 0.12$ , and  $2.06 \pm 0.13$ , respectively. Changes in  $V_{\max}$  were not statistically significant between the groups of reconstituted fibers. Because  $V_{\max}$  is considered to be influenced by the rate of XB detachment [10], our results further substantiate that Ala and Asp substitutions in RcTnI have no effect on the rate of XB detachment.

## DISCUSSION

Attempts to delineate the effects of PKA-mediated phosphorylation of cTnI on cardiac myofilament function have included approaches such as the reconstitution of mutated cTnI into fiber bundles. The use of heterologous proteins and tissues in reconstitution assays raises important issues because it amounts to multiple amino acid substitutions. This becomes a major issue in studies that are specifically designed to test the effect of minor modifications that occur during phosphorylation of proteins. Therefore, to permit an unambiguous understanding of the functional effects of PKA-mediated phosphorylation of cTnI, it is essential to minimize heterogeneity in experimental assays. We have tested the effects of Ala and Asp substitutions at Ser23/24 of cTnI using homologous proteins, so that we could attribute functional alterations solely to the changes that we engineered into cTnI. Our data provides new findings that have significant implications for interpreting data obtained from studies that use Ala and Asp substitutions in cTnI to understand the effects of PKA phosphorylation.

In agreement with previous studies [15, 16], we observed that myofilament  $Ca^{2+}$  sensitivity (as assessed by  $pCa_{50}$ ) remained unaffected when Ser23/24 of cTnI were substituted by Ala, but it decreased significantly when substituted by Asp. RcTnI S23D/24D caused a rightward shift in the  $pCa$ -tension relationship by  $\sim 0.09$   $pCa$  units (Figure 4). There was a small but significant increase in the cooperativity of tension development ( $n_H$ ) for both RcTnI S23A/24A and RcTnI S23D/24D fibers. This increase in  $n_H$  cannot be attributed to  $Ca^{2+}$ -mediated effects alone because the affinity for  $Ca^{2+}$  decreased in RcTnI S23D/24D fibers, but remained unaltered in RcTnI S23A/24A fibers. Despite this apparent increase in  $n_H$  of both Ala and Asp substitutions, a significant finding in our study is that the reconstitution of either RcTnI S23A/24A or RcTnI S23D/24D caused a significant decrease in  $Ca^{2+}$ -activated maximal tension and ATPase activity (Figure 2). This finding indicates that substitutions at Ser23/24 of cTnI, be it with an aliphatic Ala or with a negatively-charged Asp, produced a similar effect on maximal activation. Given the important role played by these amino acids in phosphorylation-mediated regulation of cardiac thin filaments, it is reasonable to posit that Ser23/24 are structurally sensitive sites in cTnI. Any modification of such structurally sensitive sites will have structural or functional consequences. For example, a previous study demonstrated that both PKC phosphorylation of Ser175 and a non-phosphorylatable Ser175Ala substitution in calponin produced a similar amount of decrease in the binding affinity of calponin to actin, suggesting that Ala substitution is not always a 'silent substitution' and that such substitutions must be used with caution [32].

There is a significant discrepancy between our observations and other studies [15, 16], which showed no effect on  $Ca^{2+}$ -activated maximal tension. Our study with Asp substitutions showed a shift of 0.09  $pCa$  units for myofilament  $Ca^{2+}$  sensitivity, while the study of Dohet et al [16] showed a shift of 0.16  $pCa$  units. We believe that such discrepancy



is probably related to the use of heterologous proteins in previous studies. For example, Zhang et al [15] reconstituted detergent-skinned porcine cardiac fibers with bovine cTnC and mouse cTnI containing Ala substitutions at Ser23/24. In a similar study, Dohet et al [16] reconstituted skinned porcine cardiac fibers with human cTnC and human cTnI containing Asp substitutions at Ser23/24. A sequence comparison between porcine cTnI vs. mouse cTnI and porcine cTnI vs. human cTnI reveals that porcine cTnI differs from mouse cTnI by 18 amino acids and from human cTnI by 15 amino acids, respectively. Furthermore, sequence comparison also reveals that the differences are not just confined to the N-terminus, but are scattered along the entire length of the cTnI protein. This suggests that the use of heterologous proteins in previous studies [15, 16] may have, in part, contributed to the observed discrepancies. The discrepancies may also result from differences in the procedures employed for extraction and reconstitution of the endogenous Tn subunits. For example, vanadate treatment was used to extract endogenous cTnI and cTnC in the studies of Zhang et al [15]. A combination of CDTA and trifluoperazine was used to extract endogenous cTnC and was followed by vanadate treatment to extract endogenous cTnI in the studies of Dohet et al [16]. Other factors, such as differences in the ionic strength of the maximal  $\text{Ca}^{2+}$  activation solution (180 mM in our study vs. 150 mM in Zhang et al [15] or 120 mM in Dohet et al [16]), and SL (2.2  $\mu\text{m}$  in our study vs. 2.0  $\mu\text{m}$  in the study of Dohet et al [16]) might have also contributed to the discrepancy.

The first question that should be addressed is, “how do Ala and Asp substitutions at Ser23/24 of cTnI lead to decreased maximal tension and ATPase activity?” It is possible that the decrease in tension and ATPase activity observed in our studies may have resulted from a decrease in the number of force-generating crossbridges (XBs). To assess this possibility, we measured the magnitude of instantaneous muscle fiber stiffness ( $E_D$ ) caused by a sudden change in muscle length during steady-state  $\text{Ca}^{2+}$  activation. A decrease in  $E_D$  of fibers reconstituted with Ala or Asp substitutions in cTnI (Figure 3) correlated well with an observed decrease in  $\text{Ca}^{2+}$ -activated maximal tension. Because  $E_D$  is proportional to the number of strongly-bound XBs [27], a significant drop in  $E_D$  suggests that the decrease in  $\text{Ca}^{2+}$ -activated tension is due to a reduced number of XBs. This suggests that the thin filament activation is reduced by Ala or Asp substitutions in cTnI. The following experimental observations give us confidence in concluding that it is the substitutions at Ser23/24 that is responsible for the attenuated activation. First, various Tn subunits incorporated equally in different groups of fibers. Second, the  $\text{Ca}^{2+}$ -activated maximal tension, ATPase activity, and  $E_D$  were attenuated in fibers reconstituted with modified cTnI, when compared to fibers reconstituted with wild-type cTnI. Because the thin filament activation depends on tightly-controlled allosteric interactions among proteins, we believe that Ala and Asp substitutions may have caused some alterations in cTnI structure, leading to decreased thin filament activation.

There is experimental evidence to show that charge modifications of cTnI lead to altered intra- and inter-molecular interactions. Altered intra-molecular interactions were observed using NMR studies [3], which demonstrated that incorporation of phosphate groups at Ser23/24 induced interactions between the side chains of Ser24 and other amino acids in cTnI. Evidence for altered inter-molecular interactions was provided by studies of Liao et al [5] and Chandra et al [33], which demonstrated that PKA-mediated phosphorylation of cTnI decreased the affinity of cTnI for cTnC. Further evidence for altered inter-molecular interactions was provided by NMR studies [14], which demonstrated that Asp substitutions at Ser23/24 of cTnI induced a closed and inactive conformation in the regulatory domain of cTnC. Although our CD spectral studies (Table 1) showed no major effects of Ala and Asp substitutions on the overall secondary structures of cTnI, it is important to note that CD spectral studies may not reveal subtle structural changes that have the potential to alter the function of a protein.

The catalytic subunit of PKA has been used in skinned rat cardiac muscle fiber studies [6, 8–10] to determine whether enhanced relaxation, following  $\beta$ -adrenergic stimulation, is a result of enhanced XB detachment kinetics. However, previous studies were inconclusive in showing an effect of cTnI phosphorylation on the rate of XB detachment. For example, de Tombe and Stienen [8] showed an unaltered tension cost (measure of XB detachment), while Saeki et al [6] showed an increase in tension cost upon PKA treatment. Previous studies have also used unloaded shortening velocity ( $V_0$ ) measurements to determine if PKA enhances XB detachment kinetics. However, some studies have shown that PKA increases XB detachment kinetics [6, 10, 34], whereas, other studies have shown no effect of PKA on XB detachment kinetics in cardiac muscle preparations [9, 35]. We measured tension cost (Figure 5A), XB detachment kinetics (Figure 5B), and  $V_{max}$  to test the effect of Ala and Asp substitutions on XB detachment kinetics. Our measurement of tension cost, XB detachment kinetics, and  $V_{max}$  showed no effect of Ala and Asp substitutions on XB detachment kinetics. Thus, our data suggest that the non-phosphorylatable Ala and phosphorylation mimicking Asp substitutions in cTnI do not alter the rate of XB detachment.

In summary, we provide diverse experimental evidence to show that Ala and Asp substitutions in cTnI lead to altered cardiac thin filament activation. Our experiments add the following new important information to the existing literature on the effects of Ala and Asp substitutions in cTnI on cardiac function: 1. Ala and Asp substitutions in cTnI reduce thin filament activation in reconstituted rat cardiac papillary muscle fibers; and 2. Ala and Asp substitutions in cTnI have no effect on the rate of XB detachment. Thus, our results have significant implications for interpreting studies that use Ala and Asp substitutions to understand how PKA phosphorylation of cTnI modulates cardiac muscle function.

## Acknowledgments

We thank Traci Topping for technical assistance with CD spectral measurements. This work was supported by National Heart, Lung, and Blood Institute Grant R01-HL-075643 (to Murali Chandra) and Poncin Scholarship (to Ranganath Mamidi).

## Abbreviations used

<b>PKA</b>	protein kinase A
<b>cTnI</b>	cardiac troponin I
<b>XB</b>	crossbridge
<b>cTnC</b>	cardiac troponin C
<b>cMyBP-C</b>	cardiac myosin binding protein-C
<b>TG</b>	transgenic
<b>BDM</b>	2, 3-butanedione monoxime
<b>A2P5</b>	diadenosine pentaphosphate
<b>SL</b>	sarcomere length
<b>CD</b>	circular dichroism

## References

1. Layland J, Solaro RJ, Shah AM. *Cardiovasc Res.* 2005; 66:12–21. [PubMed: 15769444]
2. Solaro RJ, Moir AJ, Perry SV. *Nature.* 1976; 262:615–617. [PubMed: 958429]

3. Quirk PG, Patchell VB, Gao Y, Levine BA, Perry SV. *FEBS Lett.* 1995; 370:175–178. [PubMed: 7656971]
4. Fentzke RC, Buck SH, Patel JR, Lin H, Wolska BM, Stojanovic MO, Martin AF, Solaro RJ, Moss RL, Leiden JM. *J Physiol.* 1999; 517(Pt 1):143–157. [PubMed: 10226156]
5. Liao R, Wang CK, Cheung HC. *Biochemistry.* 1994; 33:12729–12734. [PubMed: 7918499]
6. Saeki Y, Kobayashi T, Minamisawa S, Sugi H. *J Mol Cell Cardiol.* 1997; 29:1655–1663. [PubMed: 9220351]
7. Turnbull L, Hoh JF, Ludowyke RI, Rossmannith GH. *J Physiol.* 2002; 542:911–920. [PubMed: 12154188]
8. de Tombe PP, Stienen GJ. *Circ Res.* 1995; 76:734–741. [PubMed: 7728989]
9. Hofmann PA, Lange JH 3rd. *Circ Res.* 1994; 74:718–726. [PubMed: 8137507]
10. Strang KT, Sweitzer NK, Greaser ML, Moss RL. *Circ Res.* 1994; 74:542–549. [PubMed: 8118962]
11. Kentish JC, McCloskey DT, Layland J, Palmer S, Leiden JM, Martin AF, Solaro RJ. *Circ Res.* 2001; 88:1059–1065. [PubMed: 11375276]
12. Takimoto E, Soergel DG, Janssen PM, Stull LB, Kass DA, Murphy AM. *Circ Res.* 2004; 94:496–504. [PubMed: 14726477]
13. Pi Y, Kemnitz KR, Zhang D, Kranias EG, Walker JW. *Circ Res.* 2002; 90:649–656. [PubMed: 11934831]
14. Sakthivel S, Finley NL, Rosevear PR, Lorenz JN, Gulick J, Kim S, VanBuren P, Martin LA, Robbins J. *J Biol Chem.* 2005; 280:703–714. [PubMed: 15507454]
15. Zhang R, Zhao J, Potter JD. *J Biol Chem.* 1995; 270:30773–30780. [PubMed: 8530519]
16. Dohet C, al-Hillawi E, Trayer IP, Ruegg JC. *FEBS Lett.* 1995; 377:131–134. [PubMed: 8543035]
17. Chandra M, Tschirgi ML, Ford SJ, Slinker BK, Campbell KB. *Am J Physiol Regul Integr Comp Physiol.* 2007; 293:R1595–1607. [PubMed: 17626127]
18. Chandra M, Tschirgi ML, Rajapakse I, Campbell KB. *Biophys J.* 2006; 90:2867–2876. [PubMed: 16443664]
19. Montgomery DE, Tardiff JC, Chandra M. *J Physiol.* 2001; 536:583–592. [PubMed: 11600691]
20. Tardiff JC, Factor SM, Tompkins BD, Hewett TE, Palmer BM, Moore RL, Schwartz S, Robbins J, Leinwand LA. *J Clin Invest.* 1998; 101:2800–2811. [PubMed: 9637714]
21. Chandra M, Montgomery DE, Kim JJ, Solaro RJ. *J Mol Cell Cardiol.* 1999; 31:867–880. [PubMed: 10329214]
22. Placek BJ, Gloss LM. *Biochemistry.* 2002; 41:14960–14968. [PubMed: 12475245]
23. Whitmore L, Wallace BA. *Nucleic Acids Res.* 2004; 32:W668–673. [PubMed: 15215473]
24. Whitmore L, Wallace BA. *Biopolymers.* 2008; 89:392–400. [PubMed: 17896349]
25. Chandra M, Tschirgi ML, Tardiff JC. *Am J Physiol Heart Circ Physiol.* 2005; 289:H2112–2119. [PubMed: 15994854]
26. Fabiato A, Fabiato F. *J Physiol (Paris).* 1979; 75:463–505. [PubMed: 533865]
27. Ford SJ, Chandra M, Mamidi R, Dong W, Campbell KB. *J Gen Physiol.* 2010; 136:159–177. [PubMed: 20660660]
28. Lin DC, Nichols TR. *J Biomech Eng.* 2003; 125:132–140. [PubMed: 12661207]
29. Chandra M, Mamidi R, Ford S, Hidalgo C, Witt C, Ottenheijm C, Labeit S, Granzier H. *J Biol Chem.* 2009; 284:30889–30896. [PubMed: 19736309]
30. Brenner B. *Proc Natl Acad Sci U S A.* 1988; 85:3265–3269. [PubMed: 2966401]
31. Campbell KB, Chandra M, Kirkpatrick RD, Slinker BK, Hunter WC. *Am J Physiol Heart Circ Physiol.* 2004; 286:H1535–1545. [PubMed: 15020307]
32. Jin JP, Walsh MP, Sutherland C, Chen W. *Biochem J.* 2000; 350(Pt 2):579–588. [PubMed: 10947974]
33. Chandra M, Dong WJ, Pan BS, Cheung HC, Solaro RJ. *Biochemistry.* 1997; 36:13305–13311. [PubMed: 9341222]
34. Tong CW, Stelzer JE, Greaser ML, Powers PA, Moss RL. *Circ Res.* 2008; 103:974–982. [PubMed: 18802026]
35. de Tombe PP, ter Keurs HE. *Circ Res.* 1991; 68:382–391. [PubMed: 1825034]

### Highlights

- Homologous proteins were used for reconstitution in our functional assay
- Ala/Asp substitutions were introduced at Ser23/24 of cardiac troponin I (cTnI)
- Protein kinase A phosphorylation was mimicked using Asp substitutions in cTnI
- Ala/Asp substitutions at Ser23/24 of cTnI decreased the thin filament activation
- Ca<sup>2+</sup> sensitivity decreased with Asp substitutions, but not with Ala substitutions

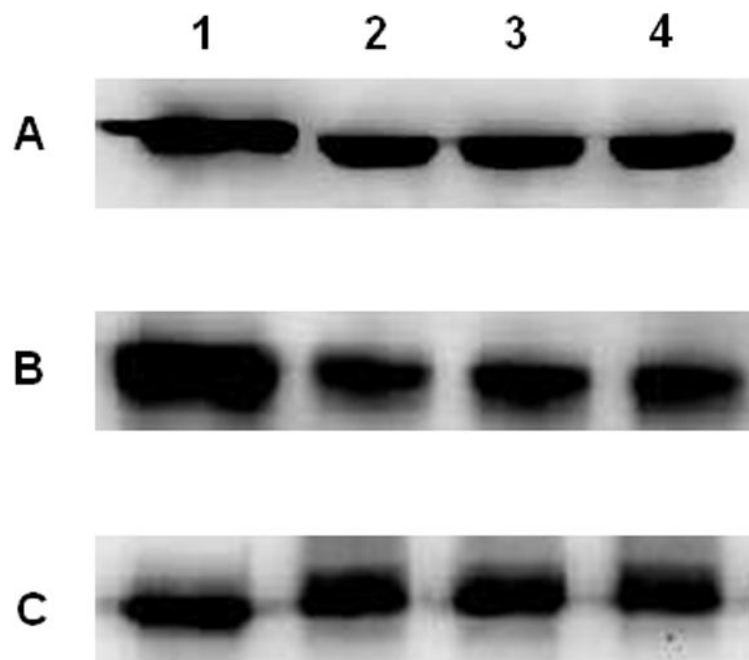


**Figure 1. Western blot analysis of Tn components in reconstituted fibers**

Panels A, B, and C indicate Western blot analysis for *c-myc* RcTnT, RcTnI, and RcTnC in reconstituted rat cardiac fibers, respectively. Lane 1 in panels A, B, and C represents purified recombinant *c-myc* RcTnT, RcTnI, and RcTnC, respectively. Lanes 2, 3, and 4 in each panel indicate samples from control RcTnI WT, RcTnI S23A/24A, and RcTnI S23D/24D reconstituted fibers, respectively. (A) Antibody to *c-myc* epitope was used to assess the incorporation of *c-myc* RcTnT into reconstituted fibers. (B) Antibody to cTnI was used to assess the incorporation of RcTnI into reconstituted fibers. (C) Antibody to cTnC was used to assess the incorporation of RcTnC into reconstituted fibers. Image J software was used to compare protein band intensities in lanes 3 and 4 to that in lane 2. The relative incorporation of *c-myc* RcTnT, RcTnI, and RcTnC was similar in all groups of fibers.

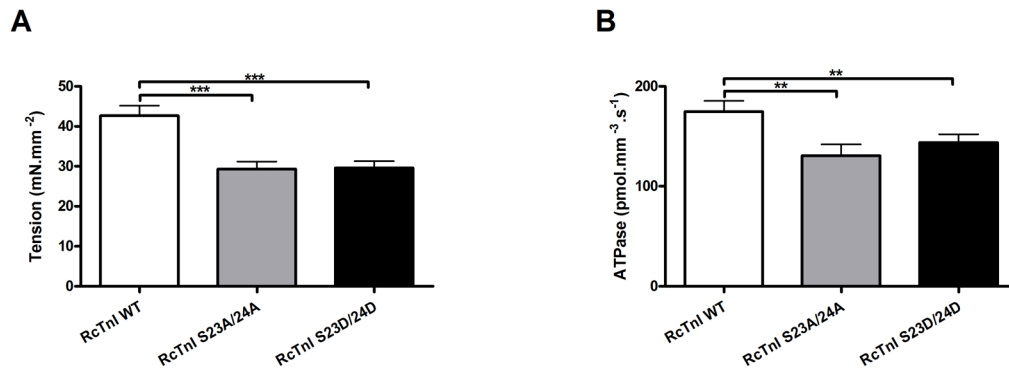


**Figure 2. Ca<sup>2+</sup>-activated maximal tension and ATPase activity in reconstituted fibers at SL 2.2  $\mu$ m**

Ca<sup>2+</sup>-activated maximal tension and ATPase activity were measured in reconstituted rat cardiac fibers at pCa 4.3 [8]. (A) Effect of RcTnI S23/24 substitutions on Ca<sup>2+</sup>-activated maximal tension in reconstituted fibers. (B) Effect of RcTnI S23/24 substitutions on Ca<sup>2+</sup>-activated maximal ATPase activity in reconstituted fibers. Substitutions at S23/24 of cTnI - be it Ala or Asp - lead to a significant decrease in Ca<sup>2+</sup>-activated maximal tension and ATPase activity. Number of determinations was at least 10 for each group. Values are reported as mean  $\pm$  SEM. \*\*\* P < 0.001, and \*\* P < 0.05.

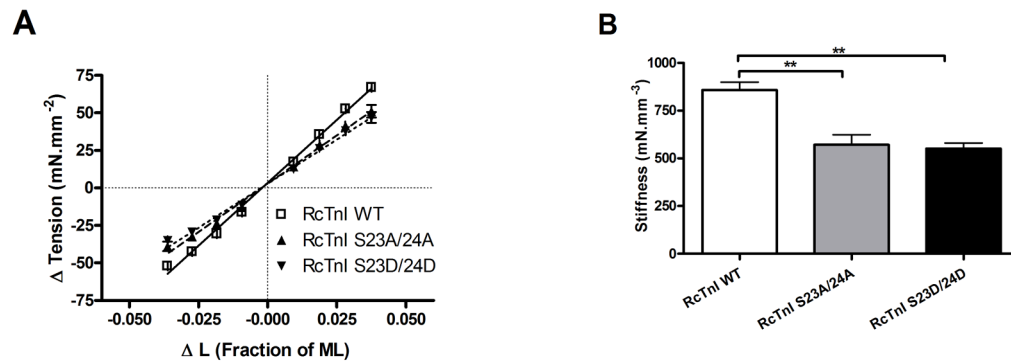


**Figure 3. Stiffness relationship and magnitude of muscle fiber stiffness in reconstituted fibers** Constantly-activated muscle fibers were subjected to step-like length changes [27]. (A) Stiffness relationships estimated from instantaneous tension responses to step-like length changes in fibers reconstituted with RcTnI WT, RcTnI S23A/24A, or RcTnI S23D/24D. The slope of relationship between changes in tension due to stretch or release ( $\Delta$ Tension) and changes in muscle length ( $\Delta L$ ) provides a measurement of muscle fiber stiffness. (B) The magnitude of muscle fiber stiffness ( $E_D$ ), determined from the slope of stiffness relationships, in fibers reconstituted with RcTnI WT, RcTnI S23A/24A, or RcTnI S23D/24D.  $E_D$ , which is a measure of the number of strongly-bound XBs, decreased in RcTnI S23A/24A and RcTnI S23D/24D reconstituted fibers. Number of observations for each group was at least 7. Values are reported as mean  $\pm$  SEM. \*\*  $P < 0.005$ .

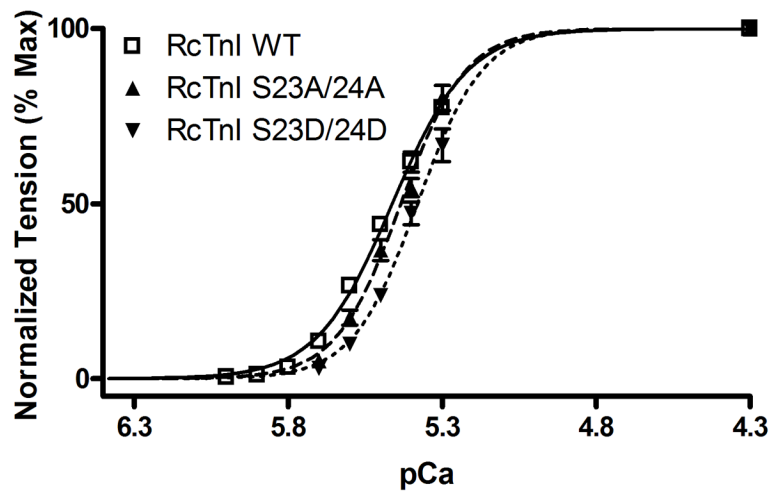


**Figure 4. Normalized pCa-tension relationships in reconstituted fibers**

Experimentally-determined sub-maximal tension values were normalized to the experimentally-determined maximal tension values at pCa 4.3. Normalized tension values were plotted against pCa to derive the pCa-tension relationships in the reconstituted fibers. The Hill equation was then fitted to the normalized pCa-tension relationships to estimate myofilament  $\text{Ca}^{2+}$  sensitivity,  $\text{pCa}_{50}$ . The curves presented are fits using the Hill equation. One-way ANOVA showed that  $\text{pCa}_{50}$  decreased significantly ( $P < 0.005$ ) in RcTnI S23D/24D reconstituted fibers, but it was unaltered in RcTnI S23A/24A reconstituted fibers. Decreased  $\text{pCa}_{50}$  in RcTnI S23D/24D reconstituted fibers is indicated by a rightward shift in the pCa-tension relationship. Number of determinations was at least 10 for each group.



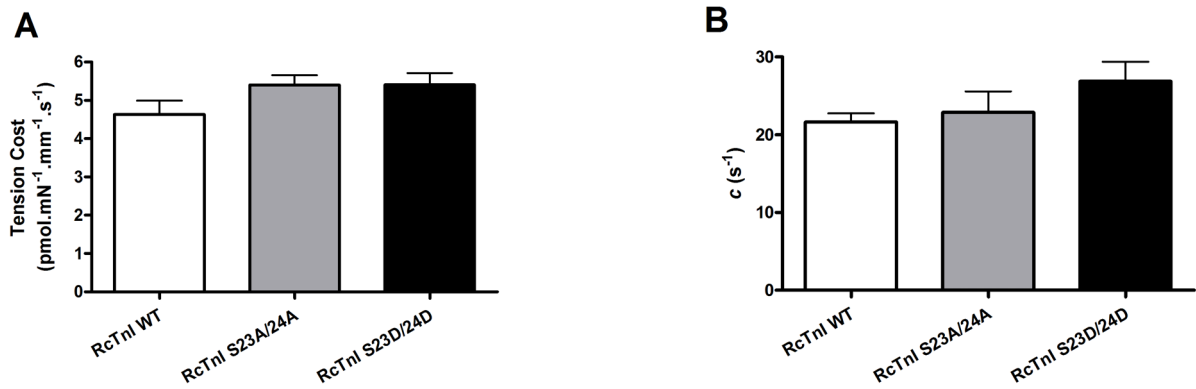


**Figure 5. Tension cost and the rate of XB distortion dynamics in reconstituted fibers**

Steady-state isometric tension and ATPase activity were measured simultaneously [8, 25]. The tension cost was derived from ATPase/tension relationship, as described previously [18]. The rate of XB distortion dynamics ( $c$ ) was estimated by fitting the NLRD model to force responses elicited by step-like changes in ML [27]. (A) Average tension cost values of the reconstituted fibers. (B) Average  $c$  values in the reconstituted fibers. Both tension cost and  $c$  represent the rate of XB detachment [31]. One-way ANOVA showed that both tension cost and  $c$  were not altered in RcTnI S23A/24A or RcTnI S23D/24D reconstituted fibers. Thus, both Ala and Asp substitutions in RcTnI did not affect the rate of XB detachment. Number of observations for each group was at least 7. Values are reported as mean  $\pm$  SEM.

**Table 1**

Secondary structural content of RcTnI, RcTnI S23A/24A, and RcTnI S23D/24D recombinant proteins estimated using far-UV CD spectral data.

	<b>RcTnI</b>	<b>RcTnI S23A/24A</b>	<b>RcTnI S23D/24D</b>
$\alpha$ -helix (%)	29.3 $\pm$ 2.8	30.7 $\pm$ 0.3	28.3 $\pm$ 0.9
$\beta$ -sheet (%)	19.0 $\pm$ 1.7	18.0 $\pm$ 0.0	17.7 $\pm$ 0.7
Random coil (%)	51.3 $\pm$ 1.5	51.0 $\pm$ 0.0	53.0 $\pm$ 0.6

Secondary structural content of the proteins was estimated by analyzing the far-UV CD spectral data using the K2D algorithm available on DICHROWEB [23]. One-way ANOVA showed no statistical differences between the percentages of  $\alpha$ -helical,  $\beta$ -sheet, and random coil contents of RcTnI S23A/24A and RcTnI S23D/24D proteins, when compared to that of RcTnI protein. Values are presented as mean  $\pm$  SEM. Number of spectra collected for each group was three.